



Research Article

Molecular-Based Identification of Actinomycetes Species That Synthesize Antibacterial Silver Nanoparticles

Abebe Bizuye ^{1,2}, Lashitew Gedamu,³ Christine Bii,⁴ Erastus Gatebe,⁵
and Naomi Maina ^{2,6}

¹Department of Medical Laboratory, College of Medicine and Health Sciences, Bahir Dar University, Bahir Dar, Ethiopia

²Molecular Biology and Biotechnology, Pan African University Institute of Basic Sciences, Innovation and Technology, Jomo Kenyatta University of Agriculture and Technology, Nairobi, Kenya

³Department of Biological Sciences, University of Calgary, Calgary, Canada

⁴Centre for Microbiology Research, Kenya Medical Research Institute, Nairobi, Kenya

⁵Kenya Industrial Research Development and Innovation, Nairobi, Kenya

⁶Department of Biochemistry, College of Health Sciences, Jomo Kenyatta University of Agriculture and Technology, Nairobi, Kenya

Correspondence should be addressed to Abebe Bizuye; hiwotabebe2015@gmail.com

Received 18 August 2020; Revised 17 October 2020; Accepted 16 November 2020; Published 24 November 2020

Academic Editor: Diriba Muleta

Copyright © 2020 Abebe Bizuye et al. This is an open access article distributed under the Creative Commons Attribution License, which permits unrestricted use, distribution, and reproduction in any medium, provided the original work is properly cited.

Infectious diseases caused by antibiotic-resistant bacteria lead to a considerable increase in human morbidity and mortality globally. This requires to search potential actinomycete isolates from undiscovered habitats as a source of effective bioactive metabolites and to synthesize metabolite-mediated antibacterial silver nanoparticles (AgNPs). The main purpose of the present study was to identify actinomycetes isolated from Thika waste dump soils that produce bioactive metabolites to synthesize antibacterial AgNPs. The synthesis of metabolite-mediated AgNP was confirmed with visual detection and a UV-vis spectrophotometer, whereas the functional groups involved in AgNP synthesis were identified using a FTIR spectrophotometer. The antibacterial activity of the metabolite-mediated AgNPs was tested by a well diffusion assay. Identification of actinomycete isolates involved in the synthesis of antibacterial AgNPs was done based on 16S rRNA gene sequence analysis. The visual detection showed that dark salmon and pale golden color change was observed due to the formation of AgNPs by KDT32 and KGT32 metabolites, respectively. The synthesis was confirmed by a characteristic UV spectra peak at 415.5 nm for KDT32-AgNP and 416 nm for KGT32-AgNP. The FTIR spectra revealed that OH, C=C, and S-S functional groups were involved in the synthesis of KDT32-AgNP, whereas OH, C=C, and C-H were involved in the formation of KGT32-AgNP. The inhibition zone results revealed that KDT32-AgNP showed 22.0 ± 1.4 mm and 19.0 ± 1.4 mm against *Escherichia coli* and *Salmonella typhi*, whereas KGT32-AgNP showed 21.5 ± 0.7 mm and 17.0 ± 0.0 mm, respectively. KDT32 and KGT32 isolates were identified as genus *Streptomyces* and their 16S rRNA gene sequences were deposited in the GenBank database with MH301089 and MH301090 accession numbers, respectively. Due to the bactericidal activity of synthesized AgNPs, KDT32 and KGT32 isolates can be used in biomedical applications.

1. Introduction

Bacteria are one of the common causative agents of infectious diseases that can be treated via antibiotics produced by secondary metabolite producing microorganisms. However, bacterial pathogens acquire resistance to antibacterial agents

through misuse and abuse of these chemicals. Acquired resistance to antibacterial can occur either by chromosomal gene mutation or by horizontal gene transfer via transduction, conjugation, and transformation [1]. These decrease the entry of antibacterial and change the antibacterial targets and metabolic inactivation of antibacterial agents [1]. These

increase human morbidity and mortality rates [2] with considerable impact on clinical and economic issues globally [3, 4].

Escherichia coli, *Salmonella* spp., *Shigella* spp., and *Vibrio* spp. are frequently occurring drug-resistant Gram-negative bacteria in the East Africa region [5]. Resistance to amoxicillin, trimethoprim-sulfamethoxazole, tetracycline, nalidixic acid, ceftriaxone, ciprofloxacin, and ofloxacin has been reported for *E. coli* isolates [6]. *Salmonella* spp. showed resistance against fluoroquinolones, ceftriaxone, ciprofloxacin, and azithromycin [7]. Moreover, most *Shigella* spp. isolated from children in the hospital showed resistance to tetracycline and trimethoprim-sulfamethoxazole [8], and this indicates the need for effective antibacterial agents.

With increasing drug-resistant pathogens against bulk antimicrobial agents, nanomedicine has attracted attention [9]. The biosorption, bioaccumulation, biomineralization, and biodegradation natures of microorganisms make them potential nanofactories [10]. Bacteria, the main group of microorganisms, are potential sources of bioactive metabolites that synthesize antibacterial AgNPs [11]. Previous reports showed that actinomycetes can produce bioactive compounds that are capable of reducing silver salts to AgNPs [12]. They are sources of diverse groups of bioactive compounds capable of synthesizing antibacterial AgNPs [13–16]. In particular, the synthesis of AgNPs by bioactive metabolites from *Streptomyces* spp. showed antibacterial activity against *E. coli* and *S. typhi* [17–20].

Actinomycetes isolated from Ethiopian and Kenyan soils produced bioactive metabolites that showed antibacterial activity against *E. coli*, *S. typhi*, and *S. boydii* [21–25]. However, the status of the synthesis of antibacterial AgNP using bioactive metabolites produced by actinomycetes isolated from the East African region is limited. The soil of waste dump sites in this region is one of the unexplored areas. Such sites may contain diverse types of nutrients (carbon source, nitrogen source, minerals, and metals such as silver) so that various bioactive metabolite producing potential actinomycetes can be found. In addition, the probability of getting antibacterial metabolites producing actinomycetes that involve the bioreduction of metals such as silver is high. The main purpose of this study was to identify actinomycete isolates isolated from Thika waste dump soil (central part of Kenya) that produce bioactive metabolites for the synthesis of antibacterial AgNPs.

2. Materials and Methods

2.1. Test Bacterial Pathogens. *Escherichia coli*, *Salmonella typhi*, and *Shigella boydii* are human bacteria pathogens used to perform *in vitro* antibacterial susceptibility tests. They are clinical isolates obtained from KEMRI (Kenya Medical Research Institute, Mycology Laboratory).

2.2. Bioactive Metabolites Preparation. KDT32 and KGT32 isolates that were isolated from composite soil samples collected from Kiganjo waste dump site in Thika, Central parts of Kenya, were used for bioactive metabolites preparation for this study. Selective isolation and bioassay-guided

screening of KDT32 and KGT32 were previously described [22].

Metabolite preparation from isolates was done according to Składanowski et al. [26]. Cell-free supernatants (secondary bioactive metabolites) were prepared by centrifugation at 5000 rpm for 25 minutes and filtration by 0.22 μm pore size filter paper from 7-day-old cultures.

2.3. Synthesis of Silver Nanoparticles, Visual Detection, and UV-Visible Spectra Analysis. The synthesis of AgNPs was done according to Składanowski et al. [26]. A mixture (1 : 1) of metabolite solution and 10 mM AgNO₃ solution was prepared from silver nitrate solution (10 mM AgNO₃ solution or 1.6987 g AgNO₃/1 L sterile distilled water) and incubated at 28°C for seven days.

The color change and absorption intensity measurement in the reaction solution at each reaction day interval was assessed through visual observation and using a 6800 double beam UV-visible spectrophotometer (Jenway, UK), respectively. UV-vis spectrophotometer was used to confirm the presence of a characteristic UV spectra peak between 400 and 500 nm. The types of AgNPs synthesized by metabolites from KDT32 and KGT32 isolates were represented as KDT32-AgNP and KGT32-AgNP, respectively.

2.4. FTIR Spectra Analysis of Biomolecules Used for AgNPs Synthesis. The sample preparation for FTIR spectra analysis of metabolite-mediated AgNPs was done according to Abd-Elnaby et al. (2016) [17]. The synthesized AgNPs were filtered using 0.22 μm pore size filter paper followed by centrifugation at 5000 rpm for 25 minutes. The pellet was washed with sterile distilled water followed by centrifugation and the supernatant was discarded. This step was repeated three times to remove unbound metabolites from metabolite-mediated nanoparticles.

The pellets were put on potassium bromide (KBr) discs and analyzed using FTIR spectrophotometer (Bruker alpha model, Germany) in transmittance mode in the range of 4000–400 cm^{-1} wavenumbers at 4 cm^{-1} resolution [27]. The results of FTIR spectra from both metabolites only and metabolite-mediated AgNPs were recorded for comparison of the band shape, band position, and band intensity change.

2.5. Testing of Antibacterial Activity of AgNPs. Both synthesized AgNPs (pellets) and the metabolites were freeze-dried to make a powder using a freeze dryer. The antibacterial activity of the metabolite-mediated AgNPs was evaluated by a well diffusion assay [10]. The pathogens (*E. coli*, *S. typhi*, and *S. boydii*) were grown overnight on Muller Hinton agar plates. The colonies were taken and suspended in 5 ml sterile water in test tubes and adjusted to 0.5 McFarland turbidity standards [28]. The suspensions were swabbed on Muller Hinton agar plates. Stock solution (2 mg/ml) was prepared from AgNO₃, KDT32-AgNPs, KGT32-AgNPs, and metabolites of KDT32 and KGT32. Streptomycin (0.1 mg/ml) and water were used as a positive and negative control, respectively. From each solution, 80 μl was

added to each well, and the plates were incubated at 37°C for 18 hrs to determine the inhibition zone.

2.6. Characterization of Isolates for Identification. Colony and cell morphology, catalase test, pH, and salt concentration tolerance test were done according to previous reports [29]. The genomic DNA of KDT32 and KGT32 was extracted and purified by the QIAamp Mini kit according to the manufacturer's instruction [30]. Amplification of 16S rRNA gene from genomic DNA of KDT32 and KGT32 isolates was done using 243F (5'-GGATGAGCCCGCGG-CCTA-3') and A3R (5'-CCAGCCCCACCTTCGAC-3') primers as described previously [31]. The quality and integrity of the amplified gene product were confirmed by gel electrophoresis according to Chen et al. [32]. The gene product was sent to Macrogen (1105AZ Amsterdam, Netherlands) and sequenced according to the manufacturer's instructions.

The quality of the obtained sequence was checked, trimmed, and prepared using BioEdit software and MEGA 7 software to get a consensus sequence. The consensus 16S rRNA gene sequence from both local isolates was submitted to GenBank to get GenBank accession number (<http://www.ncbi.nlm.nih.gov/projects/Sequin/>) using Sequin tool/program from NCBI web server [33].

Similarity search for consensus sequences was done using NCBI (<https://blast.ncbi.nlm.nih.gov/>) [32] and EzTaxon-e (<http://eztaxon-e.ezbiocloud.net/>) [34] database to get the closest reference sequences. The closest reference sequences obtained from the EzTaxon-e database were used for phylogenetic analysis using the MEGA 7 software package. Multiple sequence analysis for both reference sequences and sequences from local isolates was done using CLUSTAL W [32]. From these, character matrices and distance matrices were generated for maximum likelihood (ML) and neighbor-joining (NJ) tree construction, respectively. Neighbor joining and ML algorithm from the MEGA 7 software package were used to construct the phylogenetic tree. The tree topology (branching pattern) was validated by bootstrap values calculated by 1000 resampling replicates [32].

2.7. Data Analysis. The mean \pm standard deviation values of inhibition zone comparisons were performed using one-way ANOVA ranked with Tukey's multiple range test with descriptive analysis by SPSS version 20. The differences were tested on $p < 0.05$ (95% probability level), and all statistical values at $p < 0.05$ are statistically significantly different. The sequence similarity of KDT32 and KGT32 sequences with reference sequences was described using percentage. The taxonomic position of the isolates compared to the closest reference sequences was inferred by the construction of both character and distance matrices based on the phylogenetic tree and validated by bootstrap value.

2.8. Ethical Consideration. The antibacterial activity test was done *in vitro* against bacterial human pathogens available in KEMRI. These did not require any specific and strict permission.

3. Results

3.1. Actinomycete Metabolite-Mediated Synthesis and Characterization of Antibacterial Silver Nanoparticles

3.1.1. Visual Detection and UV-Visible Spectra Analysis of Metabolite-Mediated AgNPs. The visual and spectrophotometer detection confirmed that both KDT32 and KGT32 metabolites were successfully synthesized AgNPs (Figures 1–3). The formation of KDT32-AgNPs and KGT32-AgNPs was observed by a color change from straw to dark salmon (Figure 1(a)) and straw to a pale golden rod (Figure 1(b)), respectively.

The KDT32-AgNP and KGT32-AgNP represent a silver nanoparticle formed by KDT32 metabolite (produced by KDT32 isolate) and KGT32 metabolite (produced by KGT32 isolate), respectively.

As observed from Figures 2 and 3, there was no evidence of characteristic absorption peak scanned in the range of 400–500 nm by the reaction solution at the time of mixing and the controls (metabolite solution and AgNO₃ solution) (Figures 2 and 3). However, the reaction solution of KDT32-AgNO₃ and KGT32-AgNO₃ exhibited a clear excitation or characteristic peak after a 5-day reaction (Figures 2 and 3).

The formation of KDT32-AgNP progressively increased the absorption intensity from 1.3872 to 1.6925 as the reaction time increases from 5 to 7 days, respectively (Figure 2). A clear characteristic peak formation was observed and centered at 411.5 and 415.5 nm, respectively (Figure 2).

The KGT32-AgNPs formation also showed an increase in absorption intensity from 1.1331 to 1.3665 and decreased to 1.0114 as the reaction time increased from 5, 6 to 7 days (Figure 3). The position of the maximum spectra peaks was also shown with a minor shift center at 413.5 nm, 416 nm to 416.5 nm, respectively (Figure 3).

3.1.2. Identification of Biomolecules Used for AgNPs Synthesis Using FTIR. FTIR spectra results showed that KDT32 metabolites exhibited strong and medium absorption bands at different wavenumbers (3774.79, 3386.91, 2090.27, 1638.98, 1396.67, and 461.42 cm⁻¹) (Figure 4). The medium and sharp band at 3774.79 cm⁻¹ and the strong and broad band at 3386.91 cm⁻¹ corresponded to the O-H stretch. The medium band at 2090.27 cm⁻¹ and the strong band at 1638.98 cm⁻¹ represented -NCS (isothiocyanate) stretch and C=C (alkenes) stretch, respectively. The medium band at 1396.67 cm⁻¹ and the strong band at 461.42 cm⁻¹ represent organic sulfate stretches and stretch of S-S, respectively.

The FTIR spectra of KDT32-AgNPs results showed a change in band position, intensity, and shape compared to the spectra of KDT32 metabolite (Figure 4). This suggests the

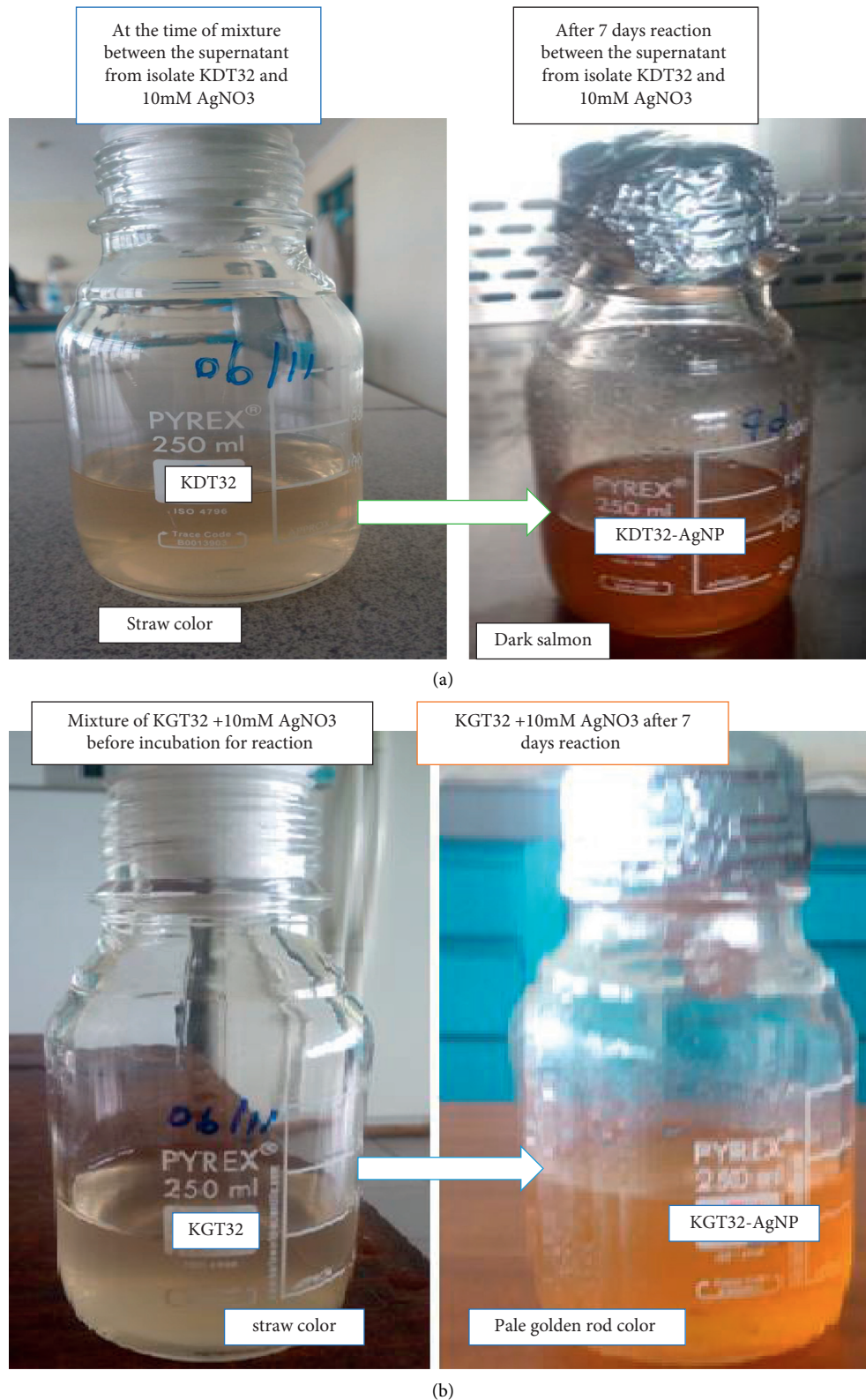


FIGURE 1: Color changes after KDT32-AgNPs (a) and KGT32-AgNPs (b) formation.

involvement of functional groups in the formation of KDT32-AgNP. FTIR spectra of KDT32-AgNPs showed a strong and broad band at 3391.31 cm^{-1} assigned to the

stretching vibration of OH. Moreover, the strong and sharp band was also observed at 1640.85 (stretching of $\text{C}=\text{C}$ -) and 445.93 cm^{-1} (stretching of S-S). The shifting of the band

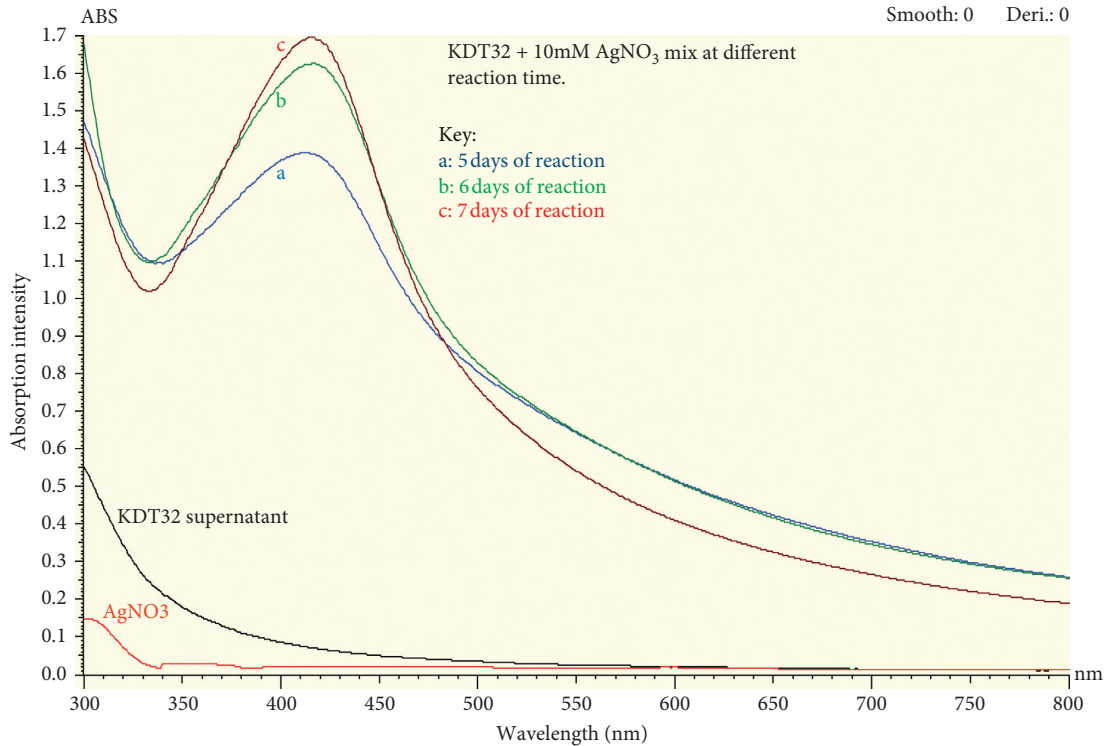


FIGURE 2: Comparison of the KDT32-AgNPs absorption intensity at maximally centered peak wavelength at different reaction days.

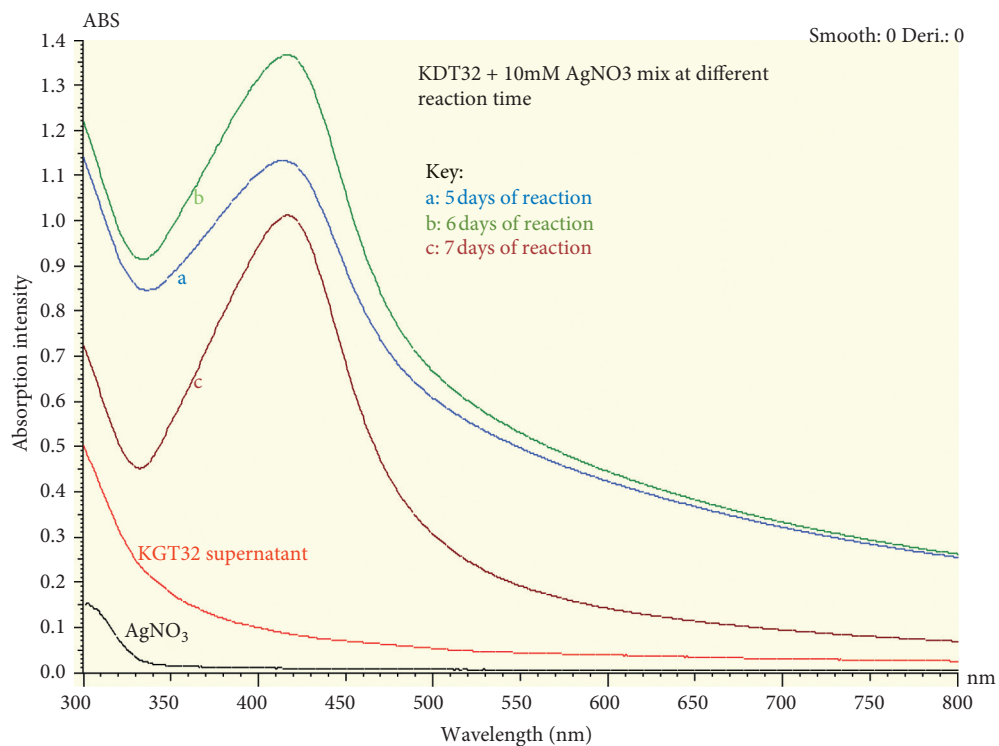


FIGURE 3: Comparison of absorption intensity of KGT32-AgNPs with respect to reaction time.

position from 3386.91 to 3391.31 cm^{-1} , 1638.98 to 1640.85 cm^{-1} , and 461.42 to 445.93 cm^{-1} may indicate the binding of the biomolecules to the AgNPs (Figure 4). These band shifts indicated that -OH, C=C, and S-S functional

groups from KDT32 metabolite were involved in the synthesis of KDT32-AgNPs.

The FTIR spectra of KGT32 metabolites showed that there were four strong bands (at 3117.76, 2074.04, 1603.98,

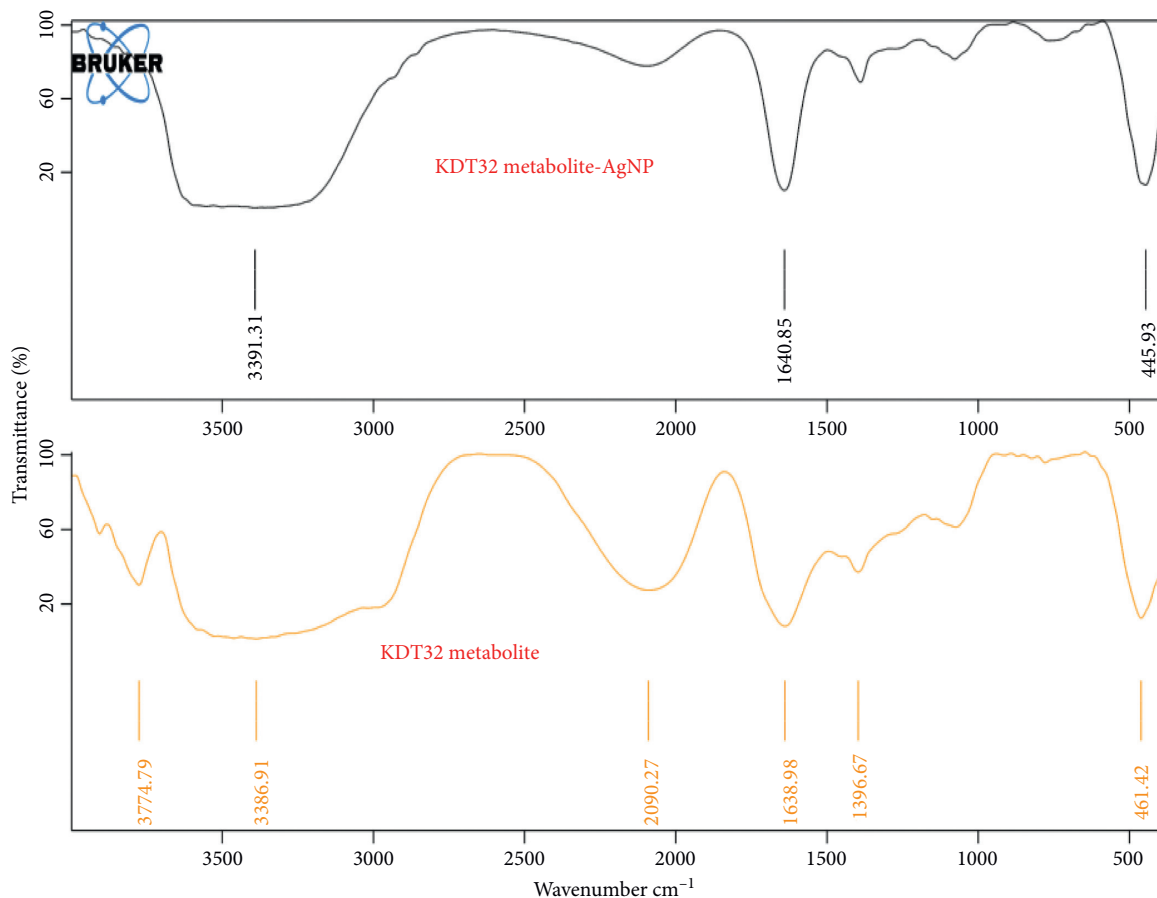


FIGURE 4: FTIR spectra comparison between the KDT32 metabolite and KDT32-AgNPs.

and 743.82 cm^{-1}) and one medium band (at 1392.90 cm^{-1}) formed (Figure 5). The bands of these wavenumbers are assigned as OH-NCS or (isothiocyanate), C=C, C-H, out plan bending, and S-S, respectively. Moreover, FTIR spectra of KGT32-AgNPs indicated that there were three strong bands observed at 3408.99 , 1639.15 , and 451.60 cm^{-1} that showed a shift in band position, shape, and intensity (Figure 5). The shifting band positions from 3117.76 to 3408.99 cm^{-1} , 1603.98 to 1639.15 cm^{-1} , and 743.82 to 451.6 cm^{-1} indicate that OH, C=C, and C-H functional groups were involved in the reduction of Ag^+ and capping of KGT32-AgNPs.

3.1.3. Antibacterial Activity Evaluation of Metabolite-Mediated AgNPs. The inhibition zone of KDT32-AgNP and KGT32-AgNPs as well as their corresponding crude extracts showed antibacterial activity against *E. coli* and *S. typhi* (Figure 6).

The inhibition zone of KDT32-AgNPs ($19.0 \pm 1.4\text{ mm}$) against *S. typhi* was higher compared to the antibacterial activity of KDT32 crude extracts ($15.0 \pm 0.0\text{ mm}$) (Table 1). Similarly, KGT32-AgNP ($17.0 \pm 0.0\text{ mm}$) showed slightly better antibacterial activity against *S. typhi* when compared to the crude extracts of KGT32 ($15.5 \pm 0.7\text{ mm}$) and AgNO_3 ($15.5 \pm 0.7\text{ mm}$) (Table 1).

3.2. Identification of Isolates KDT32 and KGT32

3.2.1. Phenotypic Characterization of Isolates KDT32 and KGT32. The KDT32 and KGT32 colony color was light yellow and white, respectively (Figure 7 and Table 2). The colony shape and texture of both isolates were circular and hard, respectively. Both local isolates were Gram-positive bacteria with filamentous cellular shape and produced catalase enzyme (Figure 7 and Table 2).

The KDT32 and KGT32 isolates grew at a pH range of 6–12 and 5–12, respectively, and they also grew at 0–7% and 0–9% NaCl concentrations, respectively (Table 2).

3.2.2. Analysis of Amplified 16S rRNA Gene Product. The gel result confirmed that the band of amplified product of KDT32 and KGT32 was between 1000 and 2000 bp size (Figure 8).

3.2.3. Sequence Analysis for Identification of KDT32 and KGT32 Isolates. The GC (Guanine-Cytosine) content for the KDT32 and KGT32 sequence was 58.32% and 59.6%, respectively (Table 3). NCBI-BLASTn similarity search showed that there were multiple hits to members of *Streptomyces* species for both isolates. The first top hit that showed similarity to the KDT32 sequence was the sequence from *Streptomyces* sp. MBE174 (AB873097.1) (Figure 9). KDT32

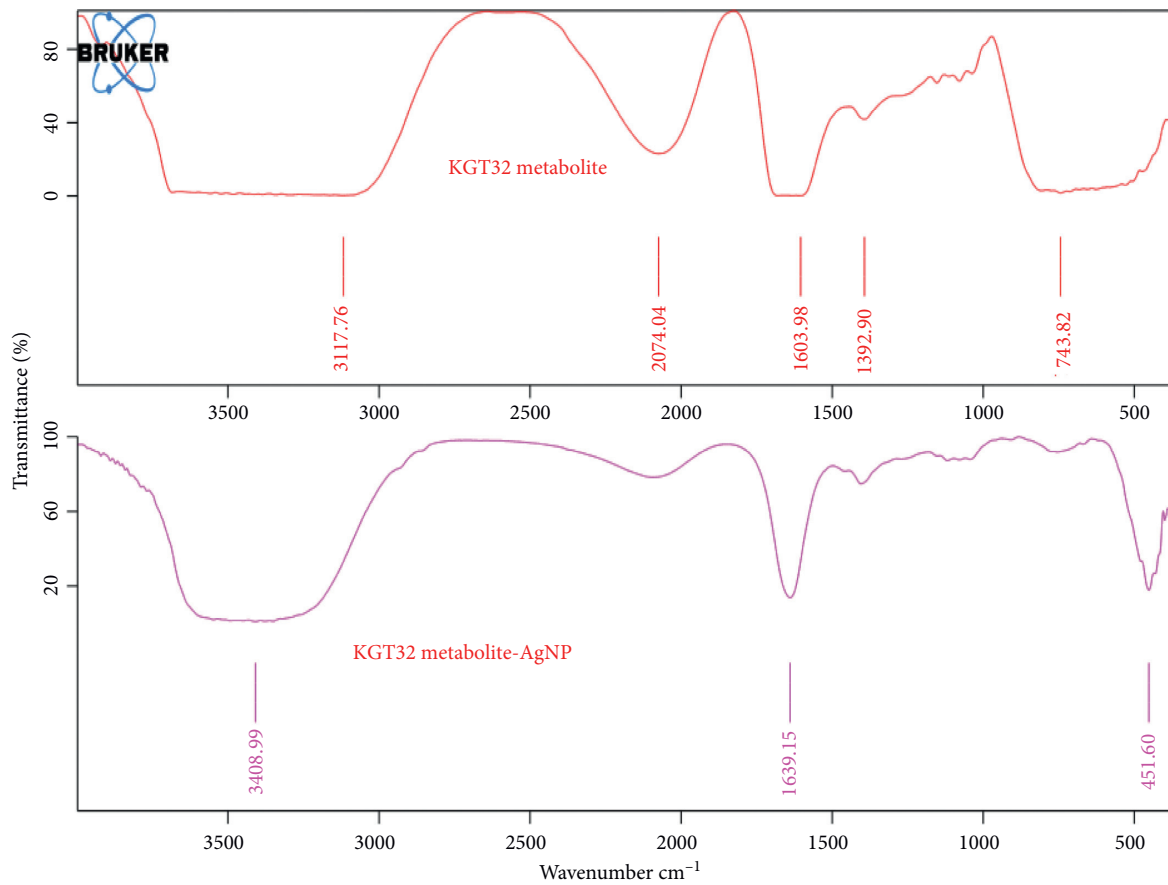
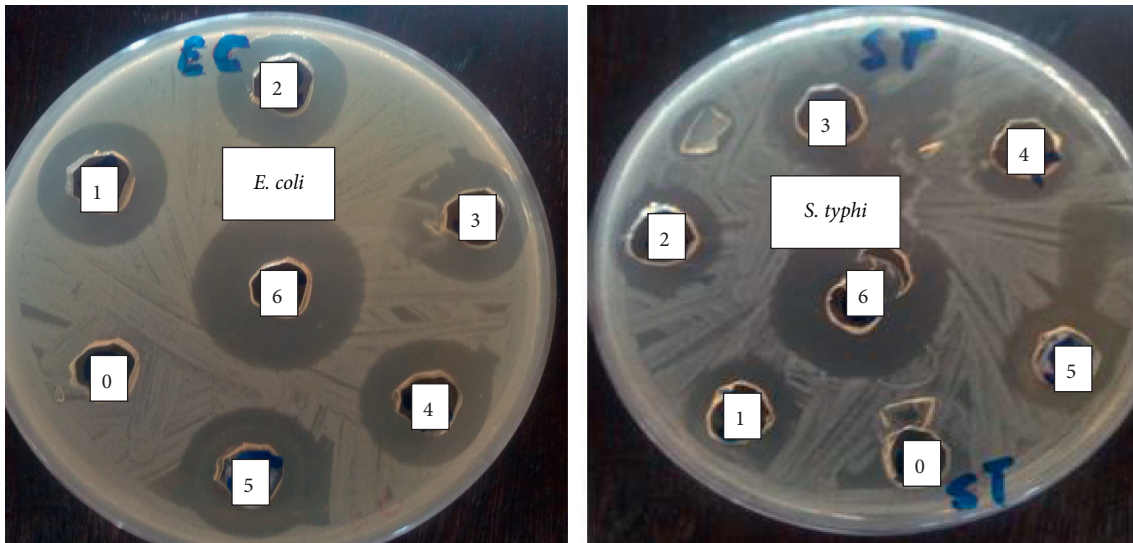


FIGURE 5: Comparison of the FTIR spectra of KGT32 metabolite and KGT32-AgNPs.



Key: 0 (negative control)

1 (KDT32 metabolite)

2 (KDT32 metabolite)

3 (KDT32 metabolite)

4 (KDT32-AgNP)

5 (AgNO₃)

6 (Streptomycin)

FIGURE 6: The bioactivity of silver nanoparticles against *E. coli* and *S. typhi*.

TABLE 1: Evaluation of the antibacterial activity of actinomycete metabolite-mediated AgNPs against selected bacteria pathogens.

Bioactivity	Inhibition zone (mm) against selected bacterial pathogens		
	<i>E. coli</i>	<i>S. typhi</i>	<i>S. boydii</i>
KDT32	19.0 ± 1.4 ^b	15.5 ± 0.7 ^c	0 ± 0.0 ^c
KGT32	20.5 ± 0.7 ^b	15.0 ± 0.0 ^c	0 ± 0.0 ^c
KDT32-AgNPs	22.0 ± 1.4 ^b	19.0 ± 1.4 ^b	0 ± 0.0 ^c
KGT32-AgNPs	21.5 ± 0.7 ^b	17.0 ± 0.0 ^{bc}	0 ± 0.0 ^c
AgNO ₃	20.5 ± 0.7 ^b	15.5 ± 0.7 ^c	11.0 ± 0.0 ^b
STP	29.0 ± 1.4 ^a	25.5 ± 0.7 ^a	25.5 ± 0.7 ^a
Negative control	0 ± 0.0 ^c	0 ± 0.0 ^d	0 ± 0.0 ^c

STP (streptomycin or positive control), sterile water (negative control), and 0 (no activity observed). Values are means ± SD. The values not sharing a common superscript letter ($a > b > c > d$) in the same column are significantly different at $p < 0.05$.

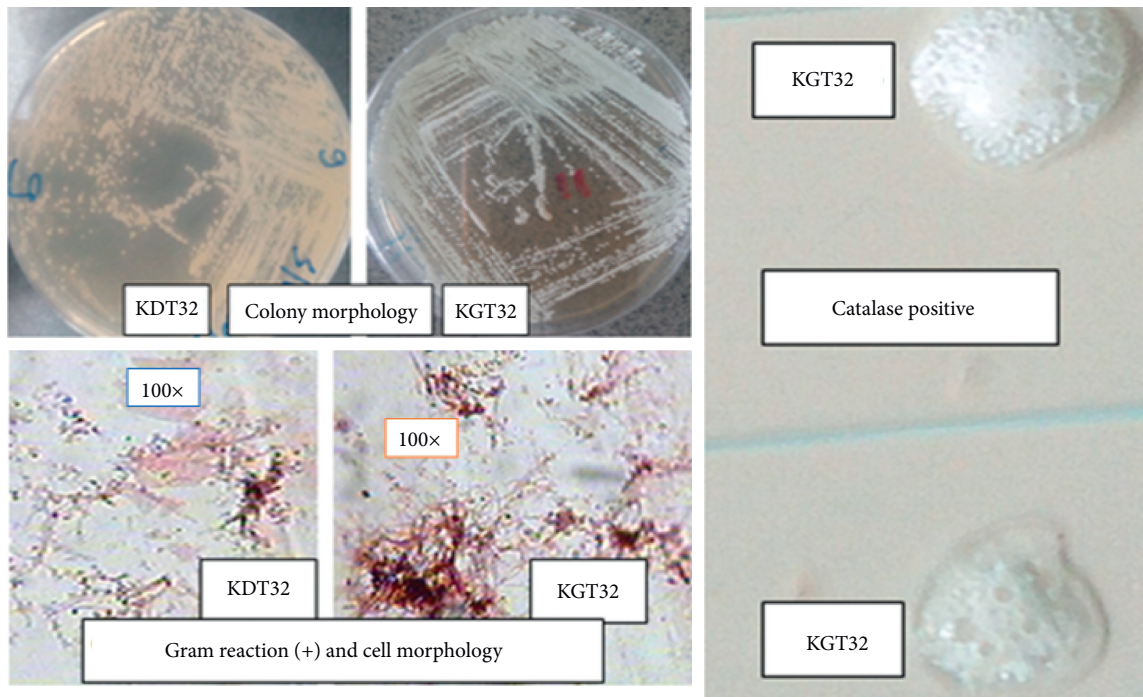


FIGURE 7: The morphology and catalase activity of KDT32 and KGT32 isolates.

TABLE 2: The phenotypic characterization of KDT32 and KGT32 isolates.

Characteristics	KDT32	KGT32
Colony Color	Light yellow	White
Colony Shape (form)	Circular	Circular
Colony Texture	Hard to scoop	Hard to scoop
Gram reaction	Positive	Positive
Cell shape	Filamentous	Filamentous
Catalase test	Positive	Positive
Growth pH range	6–12	5–12
Growth salt range	0–7%	0–9%

sequence similarity and coverage with *Streptomyces* sp. MBE174 showed 99% and 100%, respectively (Table 3). The pairwise alignment result showed that the KDT32 sequence was almost aligned base to base with *Streptomyces* sp. MBE174 sequence between the subject nucleotide position (coordinate) 417 and 1401 (Figure 10). However, there was a

gap observed at 1378 nucleotide position of *Streptomyces* sp. MBE174 sequence and T nucleotide were seen at nucleotide position 961 of the KDT32 sequence (Figure 10).

Streptomyces sp. strain SP4-AB2 (MH013316.1) was the first top closest species for KGT32 isolates (Figure 11). The KGT32 sequence was aligned with 28–975 nucleotides of *Streptomyces* sp. strain SP4-AB2 sequence (Figure 12). KGT32 sequence similarity and coverage with *Streptomyces* sp. strain SP4-AB2 sequence were 99% (946/948) and 100%, respectively. The statistics of this alignment indicated that there were 946 nucleotides aligned out of 948 (Figure 12). Thus, there were two nucleotide mismatches (2/948) between the two sequences (Table 3 and Figure 12). The first mismatch observed was a G at position 159 of the KGT32 sequence and at position 186 of *Streptomyces* sp. strain SP4-AB2 sequence, while the second mismatch was at position 866 of the KGT32 sequence and a G at position 893 of *Streptomyces* sp. strain SP4-AB2 sequence (Figure 12).

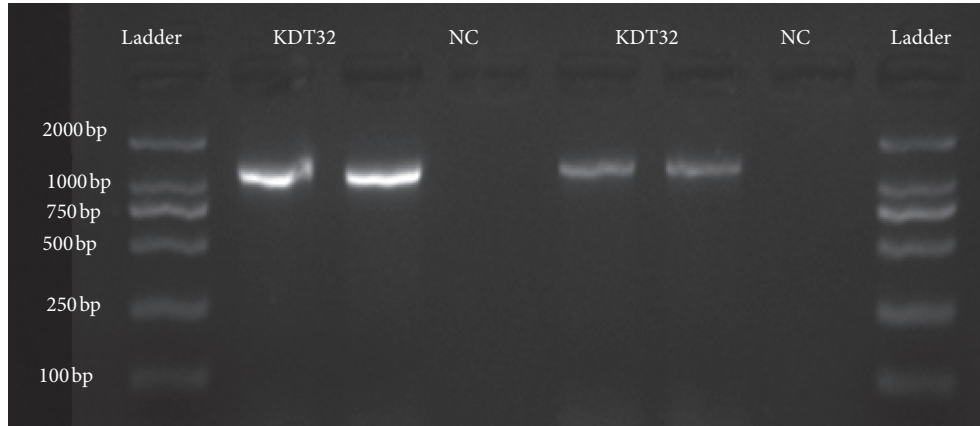


FIGURE 8: The amplified 16S rRNA gene product of KDT32 and KGT 32 isolates using 2% gel. Ladder: gel pilot mid-range ladder, 100 lanes, six fragments, 100 to 2000 bp (QIAGEN) and NC: negative control (master mix).

TABLE 3: The closest match species from GenBank database with sequences of KDT32 and KGT32 isolates.

Isolate	Accession number	Length (bp)*	GC* content (%)	Closest match	Accession number	Identity	Query coverage (%)	E-value
KDT32	MH301089	986	58.32	<i>Streptomyces</i> sp. MBE174	AB873097.1	99% (985/986)	100	0.00
KGT32	MH301090	948	59.6	<i>Streptomyces</i> sp. strain SP4-AB2	MH013316.1	99% (946/948)	100	0.00

“Isolate” is the code of our strain isolated from Thika waste damped soil “Length (bp)*” is the total size of the 16S rRNA gene sequence obtained from the isolate; “GC* content” is the ratio of Guanine and cytosine base pairs from the total sequence of our isolate: the star (*) indicates that the results were confirmed from both EzTaxon-e and NCBI-BLASTn databases; “Closest match” is the most similar species from the database to our isolate; “Accession number” is the 16S rRNA gene sequence ID of the most similar species; “Identity” is the similarity of 16S rRNA gene sequence of our isolate and the closet match species sequence; “Query coverage” is the ratio of the sequence from our isolate aligned to the closest species obtained from the database.

Sequences producing significant alignments:

Select: [All](#) [None](#) Selected: 0

Alignments [Download](#) [GenBank](#) [Graphics](#) [Distance tree of results](#)

Description	Max score	Total score	Query cover	E value	Ident	Accession
Streptomyces sp. MBE174 gene for 16S ribosomal RNA, partial sequence	1771	1771	100%	0.0	99%	AB873097.1
Streptomyces misionensis strain NIIST A2 16S ribosomal RNA, gene, partial sequence	1771	1771	100%	0.0	99%	KU695376.1
Streptomyces sp. Mem06 16S ribosomal RNA, gene, partial sequence	1771	1771	100%	0.0	99%	KR080498.1
Streptomyces hygroscopicus strain FoRh26 16S ribosomal RNA, gene, partial sequence	1771	1771	100%	0.0	99%	KM370043.1
Streptomyces sp. R21-5 gene for 16S ribosomal RNA, partial sequence	1771	1771	100%	0.0	99%	AB841957.1
Streptomyces sp. R14-5 gene for 16S ribosomal RNA, partial sequence	1771	1771	100%	0.0	99%	AB841042.1
Streptomyces sp. R9-4 gene for 16S ribosomal RNA, partial sequence	1771	1771	100%	0.0	99%	AB841027.1
Streptomyces sp. TP-A0075 gene for 16S ribosomal RNA, partial sequence	1771	1771	100%	0.0	99%	AB451554.1
Streptomyces sp. S096 16S ribosomal RNA, gene, partial sequence	1771	1771	100%	0.0	99%	EF577242.1
Streptomyces hygroscopicus subsp. hygroscopicus gene for 16S rRNA, partial sequence, strain: NBRC 3401	1771	1771	100%	0.0	99%	AB184760.1
Actinomycetales bacterium HPA160 16S ribosomal RNA, gene, partial sequence	1768	1768	100%	0.0	99%	DQ144220.1
Streptomyces misionensis strain AMA49 16S ribosomal RNA, gene, partial sequence	1766	1766	100%	0.0	99%	KX129398.1
Streptomyces sp. R4-2 gene for 16S ribosomal RNA, partial sequence	1766	1766	100%	0.0	99%	AB841004.3
Streptomyces sp. 151K0065 16S ribosomal RNA, gene, partial sequence	1766	1766	100%	0.0	99%	KX078377.1
Streptomyces misionensis strain OsiRH-1 16S ribosomal RNA, gene, partial sequence	1766	1766	100%	0.0	99%	KU321340.1
Streptomyces sp. XSRH38 16S ribosomal RNA, gene, partial sequence	1766	1766	100%	0.0	99%	KP900826.1

FIGURE 9: NCBI-BLASTn result for KDT32 16S rRNA gene sequence.

Query	1	CTTTCAGCAGGGAAGAAGCGAGAGTGACGGTACCTGCAGAAGAAGCGCCGGCTAACTACG	60
Sbjct	417	CTTTCAGCAGGGAAGAAGCGAGAGTGACGGTACCTGCAGAAGAAGCGCCGGCTAACTACG	476
Query	61	TGCCAGCAGCCGCGGTAATACGTAGGGCGCAAGCGTTGTCCGGAATTATTGGGCGTAAAG	120
Sbjct	477	TGCCAGCAGCCGCGGTAATACGTAGGGCGCAAGCGTTGTCCGGAATTATTGGGCGTAAAG	536
Query	121	AGCTCGTAGGCGGCTTGTGCGTCGGTTGTGAAAGCCCGGGCTTAACCCCGGGTCTGCA	180
Sbjct	537	AGCTCGTAGGCGGCTTGTGCGTCGGTTGTGAAAGCCCGGGCTTAACCCCGGGTCTGCA	596
Query	181	GTCGATACGGGCAGGCTAGAGTTCGGTAGGGGAGATCGGAATTCCTGGTGTAGCGGTGAA	240
Sbjct	597	GTCGATACGGGCAGGCTAGAGTTCGGTAGGGGAGATCGGAATTCCTGGTGTAGCGGTGAA	656
Query	241	ATGCGCAGATATCAGGAGGAACACCGGTGGCGAAGGCGGATCTCTGGGCCGATACTGACG	300
Sbjct	657	ATGCGCAGATATCAGGAGGAACACCGGTGGCGAAGGCGGATCTCTGGGCCGATACTGACG	716
Query	301	CTGAGGAGCGAAAGCGTGGGAGCGAACAGGATTAGATACCCTGGTAGTCCACGCCGTAA	360
Sbjct	717	CTGAGGAGCGAAAGCGTGGGAGCGAACAGGATTAGATACCCTGGTAGTCCACGCCGTAA	776
Query	361	ACGGTGGGCACTAGGTGTGGGCAACATTCACGTTGTCCGTGCCGCAGCTAACGCATTAA	420
Sbjct	777	ACGGTGGGCACTAGGTGTGGGCAACATTCACGTTGTCCGTGCCGCAGCTAACGCATTAA	836
Query	421	GTGCCCCGCCTGGGGAGTACGGCCGCAAGGCTAAAACCTCAAAGGAATTGACGGGGGCCG	480
Sbjct	837	GTGCCCCGCCTGGGGAGTACGGCCGCAAGGCTAAAACCTCAAAGGAATTGACGGGGGCCG	896
Query	481	CACAAGCGGCGGAGCATGTGGCTTAATTCGACGCAACGCGAAGAACCTTACCAAGGCTTG	540
Sbjct	897	CACAAGCGGCGGAGCATGTGGCTTAATTCGACGCAACGCGAAGAACCTTACCAAGGCTTG	956
Query	541	ACATACACCGGAAAGCATTAGAGATAGTGCCCCCTTGTGGTTCGGTGTACAGGTGGTGA	600
Sbjct	957	ACATACACCGGAAAGCATTAGAGATAGTGCCCCCTTGTGGTTCGGTGTACAGGTGGTGA	1016
Query	601	TGGCTGTCGTGAGCTCGTGTGAGATGTTGGGTAAAGTCCCGCAACGAGCGCAACCCT	660
Sbjct	1017	TGGCTGTCGTGAGCTCGTGTGAGATGTTGGGTAAAGTCCCGCAACGAGCGCAACCCT	1076
Query	661	TGTCCCGTGTGCCAGCAGGCCCTTGTGGTGTGGGACTCACGGGAGACCGCCGGGGTC	720
Sbjct	1077	TGTCCCGTGTGCCAGCAGGCCCTTGTGGTGTGGGACTCACGGGAGACCGCCGGGGTC	1136
Query	721	AACTCGGAGGAAGGTGGGACGACGTCAGTCAATGATGATGCCCCCTTATGCTTGGGCTGCAC	780
Sbjct	1137	AACTCGGAGGAAGGTGGGACGACGTCAGTCAATGATGATGCCCCCTTATGCTTGGGCTGCAC	1196
Query	781	ACGTGCTACAATGGCCGTACAATGAGCTGCGATACCGTGAGGTGGAGCGAATCTCAAAA	840
Sbjct	1197	ACGTGCTACAATGGCCGTACAATGAGCTGCGATACCGTGAGGTGGAGCGAATCTCAAAA	1256
Query	841	AGCCGGTCTCAGTTCGGATTGGGGTCTGCAACTCGACCCCATGAAGTCGGAGTCGCTAGT	900
Sbjct	1257	AGCCGGTCTCAGTTCGGATTGGGGTCTGCAACTCGACCCCATGAAGTCGGAGTCGCTAGT	1316
Query	901	AATCGCAGATCAGCATTGCTGCGGTGAATACGTTCCCGGGCCTTGTACACACCGCCCGTC	960
Sbjct	1317	AATCGCAGATCAGCATTGCTGCGGTGAATACGTTCCCGGGCCTTGTACACACCGCCCGTC	1376
Query	961	ATCGTACGAAAGTTCGGTAACACCCG 986	
Sbjct	1377	A-CGTACGAAAGTTCGGTAACACCCG 1401	

FIGURE 10: The BLAST analysis between the KDT32 (query) sequence and *Streptomyces* sp. MBE174 (AB873097.1) (sbjct = subject) sequence from the NCBI database. The nucleotide with red color indicates the difference between the query (KDT32) and the subject (*Streptomyces* sp. MBE174 (AB873097.1)) sequence.

EzTaxon-e server search results confirmed that 30 *Streptomyces* species showed 99.19%–99.8% sequence similarity to KDT32 isolate (Figure 13). *Streptomyces lavenduligriseus* strain NRRL ISP-5487 is the first top closest hit that showed 99.8% sequence similarity to KDT32 sequence (Table 4). In this case, 985/986 bp of the sequence of KDT32

was aligned between 403 and 1388 sequence of *S. lavenduligriseus* strain NRRL ISP-5487. The number of mismatch nucleotides between the sequence of KDT32 and *S. lavenduligriseus* strain NRRL ISP-5487 was 2 bps (Table 4).

Similarly, 30 *Streptomyces* species obtained from the EzTaxon-e database that showed 99.26%–99.79% sequence

Sequences producing significant alignments:

Select: [All](#) [None](#) [Selected](#)

Alignments [Download](#) [GenBank](#) [Graphics](#) [Distance tree of results](#)

Description	Max score	Total score	Query cover	E value	Ident	Accession
Streptomyces sp. strain SP4-AB2 16S ribosomal RNA gene, partial sequence	1701	1701	100%	0.0	99%	MH013316.1
Streptomyces sp. strain SP1-V4 16S ribosomal RNA gene, partial sequence	1698	1698	100%	0.0	99%	MH013308.1
Streptomyces sp. strain W2 16S ribosomal RNA gene, partial sequence	1698	1698	100%	0.0	99%	KY402227.1
Streptomyces sp. strain 49D 16S ribosomal RNA gene, partial sequence	1698	1698	100%	0.0	99%	KY214200.1
Streptomyces sp. strain Y355 16S ribosomal RNA gene, partial sequence	1698	1698	100%	0.0	99%	KX426373.1
Streptomyces sp. strain 544F 16S ribosomal RNA gene, partial sequence	1698	1698	100%	0.0	99%	KX426362.1
Streptomyces sp. strain 563F 16S ribosomal RNA gene, partial sequence	1698	1698	100%	0.0	99%	KX426360.1
Streptomyces sp. strain 562F 16S ribosomal RNA gene, partial sequence	1698	1698	100%	0.0	99%	KX426359.1
Streptomyces sp. strain 541F 16S ribosomal RNA gene, partial sequence	1698	1698	100%	0.0	99%	KX426358.1
Streptomyces sp. strain 528F 16S ribosomal RNA gene, partial sequence	1698	1698	100%	0.0	99%	KX426355.1
Streptomyces sp. strain 525F 16S ribosomal RNA gene, partial sequence	1698	1698	100%	0.0	99%	KX426354.1
Streptomyces sp. strain 10147b 16S ribosomal RNA gene, partial sequence	1698	1698	100%	0.0	99%	KX573711.1
Streptomyces sp. strain 182015P60-2 16S ribosomal RNA gene, partial sequence	1698	1698	100%	0.0	99%	KX538269.1
Streptomyces sp. JSM 147799 16S ribosomal RNA gene, partial sequence	1698	1698	100%	0.0	99%	KR817749.1
Streptomyces sp. JSM 147823 16S ribosomal RNA gene, partial sequence	1698	1698	100%	0.0	99%	KR817748.1
Streptomyces sp. JSM 147779 16S ribosomal RNA gene, partial sequence	1698	1698	100%	0.0	99%	KR817747.1

FIGURE 11: NCBI-BLAST result for KGT32 16S rRNA gene sequence.

similarities to KGT32 isolate were retrieved (Figure 9). Four strains showed 99.79% sequence similarity to the KGT32 sequence. The first most top closest species to the sequence of KGT32 was the sequence of *Streptomyces albidoflavus* strain DSM40455 (Table 4). From this, 947/948 bp of the sequence of KGT32 was aligned with 264–1211 bp range of sequence of *S. albidoflavus* strain DSM40455. The number of mismatched nucleotides between KGT32 and *S. albidoflavus* strain DSM40455 was 2/947 (Table 4). Therefore, the isolates KDT32 and KGT32 belonged to *Streptomyces* species and were deposited in the GenBank database with MH301089 and MH301090 GenBank accession numbers, respectively.

3.2.4. Molecular Phylogenetic Analysis of KDT32 and KGT32 Isolates. The sequence of KDT32 and KGT32 with sequences from 60 *Streptomyces* type strains retrieved from the EzTaxon-e database was analyzed using NJ and ML algorithms to see the taxonomic position of local isolates (Figure 13). The resulting trees showed that the local isolates were found at different taxonomic positions (Figure 13). It also confirmed that both local isolates showed a clade with different *Streptomyces* species retrieved from the EzTaxon-e database.

The result of both NJ and ML tree analysis confirmed that the KDT32 isolate formed a monophyletic clade with *Streptomyces nodosus* strain ATCC 14899 (CP009313; Figure 13). Moreover, the sequence of KDT32 and *S. nodosus* strain ATCC 14899 showed 99.79% sequence similarity (Table 4). On the other hand, KGT32 formed a distinct clade with *Streptomyces fabae* T66 (KM229360) and *Streptomyces cinerochromogenes* NBRC13822 (AB184507). The KGT32 sequence showed 99.68% and 99.58% sequence similarity with *S. fabae* T66

(KM229360) and *S. cinerochromogenes* NBRC13822 (AB184507), respectively (Figure 13). Thus, these confirmed that the local isolates that produced bioactive metabolites capable of synthesis of antibacterial silver nanoparticles were grouped under the genus *Streptomyces* species.

4. Discussion

The visual detection of the present study revealed that KDT32 metabolite-AgNO₃ and KGT32 metabolite-AgNO₃ reaction solution showed dark salmon and pale golden rod color change, respectively. These may indicate bioreduction of Ag⁺ and morphological indicators to detect the synthesis of AgNPs. The synthesis of AgNPs by cell-free filtrate from *Streptomyces rochei* MHM13 treated with AgNO₃ showed pale yellow color change [17]. In other studies, AgNPs synthesized by metabolite from *Streptomyces* sp. LK3 [35], *S. parvulus* SSNP11 [19], *Streptomyces* sp. NH21 [26], and *Streptomyces* sp. SS2 [36] showed a dark brown color change. These color changes occur due to the absorption of visible light and the effect of surface plasmon resonance on silver. The differences in color changes may be due to differences in the type of biomolecules involved in bioreduction of Ag⁺ and capping of AgNPs. These clearly indicate that KDT32 and KGT32 metabolites have the potential to reduce Ag⁺ to form AgNPs.

The absorption intensity result showed that the maximum spectra peak was centered at 415.5 nm and 416 nm for KDT32-AgNP and KGT32-AgNPs, respectively. Previous studies revealed that the typical AgNPs show maximum UV-vis spectra peaks between 400 and 500 nm, and this is a reliable criterion indicating the formation of AgNPs. Silver

Query	1	GAGGGCGACCGGCCACACTGGGACTGAGACACGGCCCAGACTCCTACGGGAGGCAGCAGT	60
Sbjct	28	GAGGGCGACCGGCCACACTGGGACTGAGACACGGCCCAGACTCCTACGGGAGGCAGCAGT	87
Query	61	GGGGAATATTGCACAATGGGCGAAAGCCTGATGCAGCGACGCCGCGTGAGGGATGACGGC	120
Sbjct	88	GGGGAATATTGCACAATGGGCGAAAGCCTGATGCAGCGACGCCGCGTGAGGGATGACGGC	147
Query	121	CTTCGGGTTGTAAACCTCTTTCAGCAGGGAAGAAGCGAAGTGCAGGTACCTGCAGAAGA	180
Sbjct	148	CTTCGGGTTGTAAACCTCTTTCAGCAGGGAAGAAGCGAAGTGCAGGTACCTGCAGAAGA	207
Query	181	AGCGCCGGCTAACTACGTGCCAGCAGCCGCGTAATACGTAGGGCGCAAGCGTTGTCCGG	240
Sbjct	208	AGCGCCGGCTAACTACGTGCCAGCAGCCGCGTAATACGTAGGGCGCAAGCGTTGTCCGG	267
Query	241	AATTATTGGGCGTAAAGAGCTCGTAGGCGGCTTGTACAGTCGGTTGTGAAAGCCGGGGC	300
Sbjct	268	AATTATTGGGCGTAAAGAGCTCGTAGGCGGCTTGTACAGTCGGTTGTGAAAGCCGGGGC	327
Query	301	TTAACCCCGGCTGCAGTCGATACGGCAGGCTAGAGTTCGGTAGGGGAGATCGGAATT	360
Sbjct	328	TTAACCCCGGCTGCAGTCGATACGGCAGGCTAGAGTTCGGTAGGGGAGATCGGAATT	387
Query	361	CCTGGTGTAGCGGTGAAATGCGCAGATATCAGGAGGAACACCGGTGGCGAAGGCGGATCT	420
Sbjct	388	CCTGGTGTAGCGGTGAAATGCGCAGATATCAGGAGGAACACCGGTGGCGAAGGCGGATCT	447
Query	421	CTGGGCCGATACTGACGCTGAGGAGCGAAAGCGTGGGGAGCGAACAGGATTAGATACCT	480
Sbjct	448	CTGGGCCGATACTGACGCTGAGGAGCGAAAGCGTGGGGAGCGAACAGGATTAGATACCT	507
Query	481	GGTAGTCCACGCCGTAAACGGTGGGCACTAGGTGTGGGCAACATTCCACGTTGTCCGTGC	540
Sbjct	508	GGTAGTCCACGCCGTAAACGGTGGGCACTAGGTGTGGGCAACATTCCACGTTGTCCGTGC	567
Query	541	CGCAGCTAACGCATTAAGTGCCCGCCTGGGGAGTACGGCCGCAAGGCTAAACTCAAAG	600
Sbjct	568	CGCAGCTAACGCATTAAGTGCCCGCCTGGGGAGTACGGCCGCAAGGCTAAACTCAAAG	627
Query	601	GAATTGACGGGGGCCCGCACAAAGCGGCGGAGCATGTGGCTTAATTTCGACGCAACGCGAAG	660
Sbjct	628	GAATTGACGGGGGCCCGCACAAAGCGGCGGAGCATGTGGCTTAATTTCGACGCAACGCGAAG	687
Query	661	AACCTTACCAAGGCTTGACATACACCGGAAACGCTCTGGAGACAGGCGCCCCCTTGTGGTC	720
Sbjct	688	AACCTTACCAAGGCTTGACATACACCGGAAACGCTCTGGAGACAGGCGCCCCCTTGTGGTC	747
Query	721	GGTGTACAGGTGGTGCATGGCTGTCGTCAGCTCGTGTCTGTGAGATGTTGGGTTAAGTCCC	780
Sbjct	748	GGTGTACAGGTGGTGCATGGCTGTCGTCAGCTCGTGTCTGTGAGATGTTGGGTTAAGTCCC	807
Query	781	GCAACGAGCGCAACCCTTGTCCCGTGTGCCAGCAGGCCCTTGTGGTGTGGGACTCAC	840
Sbjct	808	GCAACGAGCGCAACCCTTGTCCCGTGTGCCAGCAGGCCCTTGTGGTGTGGGACTCAC	867
Query	841	GGGAGACCGCCGGGTCAACTCGGAAGAAGGTGGGGACGACGTCAAGTCATCATGCCCT	900
Sbjct	868	GGGAGACCGCCGGGTCAACTCGGAAGAAGGTGGGGACGACGTCAAGTCATCATGCCCT	927
Query	901	TATGTCTTGGGCTGCACACGTGCTACAATGGGCCGGTACAATGAGCTG 948	
Sbjct	928	TATGTCTTGGGCTGCACACGTGCTACAATGGGCCGGTACAATGAGCTG 975	

FIGURE 12: The BLAST analysis between the KGT32 (query) sequence and *Streptomyces* sp. strain SP4-AB2 (sbjct = subject) sequence from the NCBI database. The nucleotide with red color indicates the difference between the query (KGT32) and the subject (*Streptomyces* sp. strain SP4-AB2) sequence.

nanoparticles synthesized by metabolites from *Streptomyces rochei* MHM13 showed a characteristic peak at 410 nm [17]. Silver nanoparticles synthesized by metabolites from *Streptomyces* sp. SS2 [36] and *Streptomyces* sp. LK3 [35] showed a characteristic peak at 420 nm. Another study showed that UV-vis spectra of AgNPs synthesized by metabolites from *Streptomyces* sp. NH21 were observed at 402 and 424 nm [26].

The functional groups involved in the synthesis of nanoparticles were identified by observing the change in FTIR spectra, band position, shape, and intensity in AgNPs compared to the spectra band of the metabolite only. The band position shift from 3386.91 to 3391.31 cm^{-1} , 1638.98 to 1640.85 cm^{-1} , and 461.42 to 445.93 cm^{-1} indicates that O-H stretch, C=C, and S-S from KDT32 metabolites were major functional groups involved in the synthesis of KDT32-

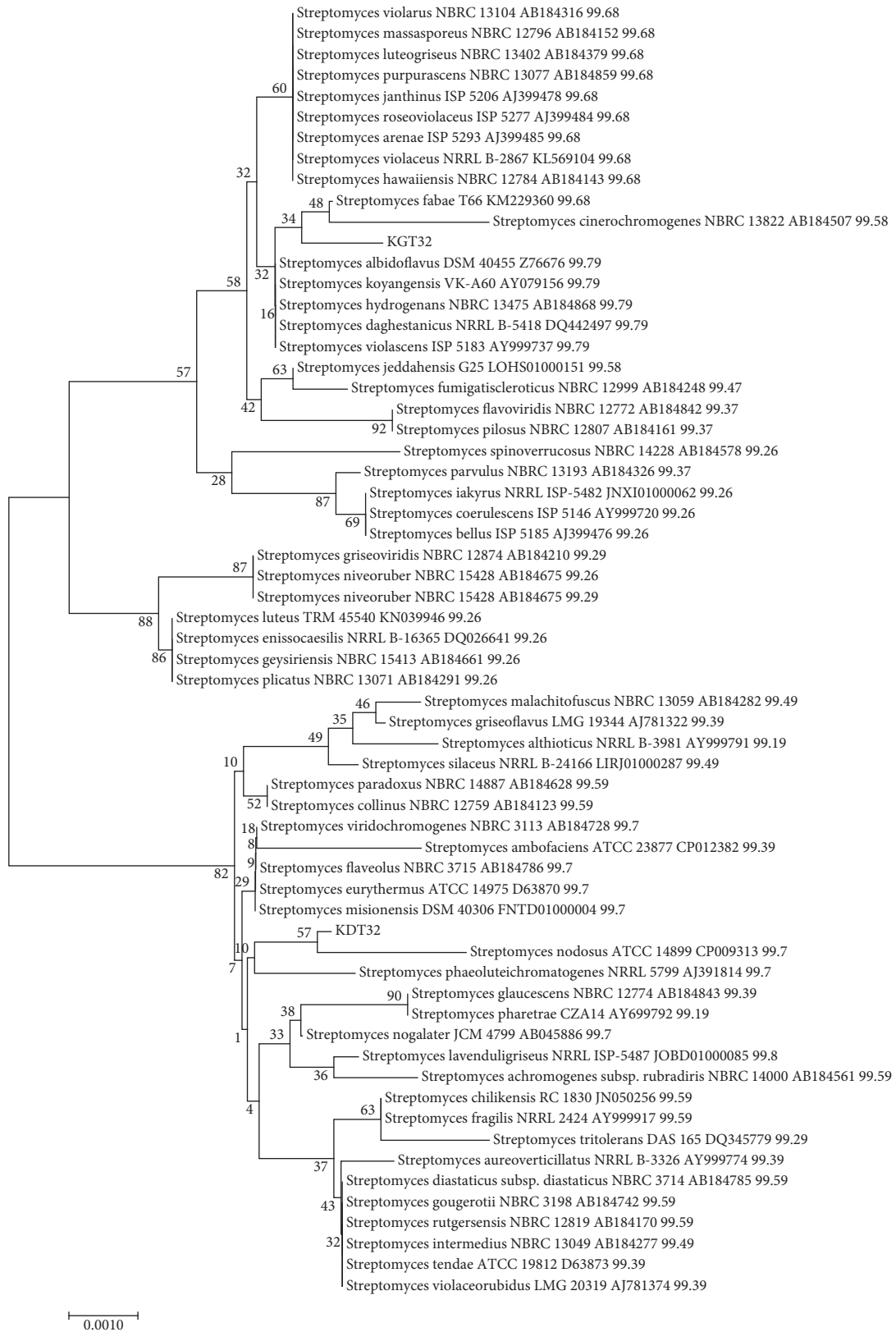


FIGURE 13: Taxonomic position and evolutionary relationship determination of KDT32 and KGT32 isolate sequences with reference sequences (strains of genus *Streptomyces*) from phylogenetic tree constructed by ML algorithm. The phylogenetic tree was validated by a bootstrap analysis (1000 replications) with values shown at branch nodes. Bar indicates substitutions per nucleotide position. Evolutionary analyses were conducted in MEGA7. *Streptomyces violarius* NBRC 13104 AB184316 99.68: *Streptomyces violarius* = taxon name; NBRC 13104 = strain type; AB184316 = GenBank accession number; 99.68 = percent of sequence similarity).

TABLE 4: The KDT32 and KGT32 sequence analysis using EzTaxon databases.

Isolate	Completeness (%)	First top hit taxon	First top hit strain ^T	Accession number	Similarity (%)	Diff/total nt	Top hit taxonomy
KDT32	68	<i>Streptomyces lavenduligriseus</i>	NRRL ISP-5487 ^T	JOBD01000085	99.8	2/985	Bacteria ^D Actinobacteria ^P Actinobacteria ^C Streptomycetales ^O Streptomycetaceae ^F Streptomyces ^G
		<i>Streptomyces albidoflavus</i>	ATCC25422 & DSM40455 ^T	Z76676	99.79	2/847	
KGT32	65.5	<i>Streptomyces koyangensis</i>	VK-A60 ^T	AY079156	99.79	2/947	Bacteria ^D Actinobacteria ^P Actinobacteria ^C
		<i>Streptomyces hydrogenans</i>	NBRC 13475 ^T	AB184868	99.79	2/947	Actinobacteria ^C Streptomycetales ^O
		<i>Streptomyces daghestanicus</i>	NRRL B-5418 ^T	DQ442497	99.79	2/946	Streptomycetaceae ^F Streptomyces ^G
		<i>Streptomyces violascens</i>	ISP 5183 ^T	AY999737	99.79	2/945	

“Completeness” is the ratio of the length of our sequence to the full-length sequence; “Top hit taxon” is the first closet species in the database; “First top hit strain^T” is the first top closet strain type; “Accession” is the ID for the closet species in the database; “Similarity” is the sequence similarity between the closet species and our isolate; “Different/total nucleotide” is the number of mismatched base pair between the closet species and our isolate from the total number of compared sequences; “Top hit taxonomy” is the taxonomical hierarchy of our isolate-based 16S rRNA gene sequence from Domain (Bacteria) to genus (*Streptomyces*) {D = domain, P = phylum, C = class, O = order, F = family, G = genus}

AgNPs. Similarly, the shift in band position from 3117.76 to 3408.99 cm^{-1} , 1603.98 to 1639.15 cm^{-1} , and 743.82 to 451.6 cm^{-1} reveals that O-H, C=C, and C-H biomolecules from KGT32 metabolites were involved in the synthesis of KGT32-AgNPs. This band peak shift alteration between the metabolite and the metabolite mediated by AgNPs shows the existence of biomolecules that were involved in the reduction of Ag^+ and capping of AgNPs. As reported, antibacterial compounds have active functional groups such as amide and hydroxyl groups to reduce Ag^+ and cap AgNPs [18]. Another study showed that the active functional group O-H (3417 cm^{-1}) [35] was involved in the reduction of Ag^+ and capping of antibacterial AgNPs. Similarly, earlier studies have reported that -OH (3384 cm^{-1}) is one of the functional groups used to reduce Ag^+ and capping of AgNPs [37]. These clearly indicate that KDT32 and KGT32 isolates are the source of metabolites having potential functional groups that reduce Ag^+ and capping AgNPs.

The bioassay study of KDT32-AgNP and KGT32-AgNP showed antibacterial activity against *E. coli* and *S. typhi*. The inhibition zone of KDT32-AgNP against *E. coli* and *S. typhi* was 22.0 ± 1.4 mm and 19.0 ± 1.4 mm, respectively. Similarly, KGT32-AgNP revealed an inhibition zone of 21.5 ± 0.7 mm and 17.0 ± 0.0 mm against *E. coli* and *S. typhi*, respectively. However, the present study showed that no antibacterial activity was observed against *S. boydii* and a similar result was reported by Chauhan et al. [18]. Earlier reports showed that AgNP synthesized by *Streptomyces rochei* MHM13 metabolite showed 16 mm and 18 mm inhibition zone against *E. coli* and *S. typhi*, respectively [17]. In another study [36], AgNP synthesized by metabolites from *Streptomyces* sp. SS2 showed 18.25 ± 1.5 mm inhibition zone against *E. coli*. Silver nanoparticles synthesized by *S. parvulus* SSNP11 metabolites showed a 26 mm inhibition zone against *S. typhi* [19]. These

clearly indicate that KDT32 and KGT32 metabolite mediated the synthesis of antibacterial AgNPs with potential bionanotechnology that can be used in biomedical applications.

The present study demonstrated that both KDT32 and KGT32 isolates were Gram positive, had filamentous cell shape, and produced catalase enzyme that grew at 6–12 and 5–12 pH values and 0–7% and 0–9% NaCl concentrations, respectively. This is in agreement with studies that antibacterial metabolites producing *Streptomyces* species isolated from soil showed growth between 4 and 12 pH and 0–7% salt concentration [38, 39].

NCBI-BLASTn search results indicate that sequence of KDT32 isolate showed 99% sequence similarity with a sequence of *Streptomyces* sp. MBE174. The biomedical and pharmaceutical application of *Streptomyces* sp. MBE174 is unknown. Moreover, based on the EzTaxon-e database search result, the sequence of KDT32 isolate showed 99.8% sequence similarity with *S. lavenduligriseus* strain NRRL ISP-5487 that produced polyene macrolides (pentenomyicine II, pentenomyicine III, and narangomyicine) [40].

Similarly, the sequences of KGT32 isolate showed 99% similarity with *Streptomyces* sp. strain SP4-AB2 (MH013316.1) with both medical and industrial roles but yet to be determined. EzTaxon-e similarity search indicated that sequence of KGT32 isolate showed 99.79% similarity with *S. albidoflavus* strain DSM40455, *S. koyangensis* strain VK-A60, *S. hydrogenans* strain NBRC 13475, *S. daghestanicus* strain NRRL B-5418, and *S. violascens* strain ISP 5183. These microbes are known in the production of different antimicrobial compounds such as paulomycin A and paulomycin B [41], 4-phenyl-3-butenoic acid [42], actinomycin D [43], and valinomycin [44], respectively. Unlike local isolates KDT32 and KGT32, a literature search about the role of these reference

Streptomyces species in nanodrug synthesis has not been reported.

The phylogenetic tree constructed from KDT32, KGT32, and reference sequences retrieved from the EzTaxon-e database revealed that the taxonomic position of both KDT32 and KGT32 isolates formed different clades with members of genus *Streptomyces*. Both NJ and ML trees inferred that the KDT32 isolate formed a monophyletic clade with *S. nodosus* strain ATCC 14899 that had 99.7% sequence similarity. *Streptomyces nodosus* is known in the production of antifungal antibiotics (polyene macrolide antibiotic, amphotericin B) [45] and other bioactive compounds (polyketides, peptides, siderophores, and terpenes) [46]. On the other hand, the KGT32 isolate formed a distinct clade with *S. fabae* strain T66 and *S. cinerochromogenes* strain NBRC13822. *Streptomyces fabae* is known for the production of antibacterial and antifungal antibiotics [47] and *S. cinerochromogenes* produced cineromycin B that has a role in antiadipocyte differentiation [48]. However, the role of these reference *Streptomyces* species in nanodrug synthesis is unknown. Thus, not only do KDT32 and KGT32 isolates produce antibacterial metabolites but also the metabolites are capable of synthesizing antibacterial AgNPs.

5. Conclusion

Bioactive metabolites from KDT32 and KGT32 isolates synthesize antibacterial AgNP (KDT32-AgNP and KGT32-AgNP) against *E. coli* and *S. typhi* but not against *S. boydii*. Due to its bactericidal activity of the synthesized AgNPs, hence, KDT32 and KGT32 metabolites can be used for antibacterial activity in different biomedical applications. The KDT32 and KGT32 isolates that produce bioactive metabolites to synthesize antibacterial AgNPs were identified as *Streptomyces* species.

Data Availability

The data used to support the findings of this study are included within the article.

Conflicts of Interest

The authors declare no conflicts of interest.

Acknowledgments

This research work was funded by the African Union Commission (ADF/BD/WP/2013/68 to CNM) and Japanese International Co-operation Agency (JICA) (00025 to CNM), and the authors also thank the institutes. The authors are also grateful to PAUISTI Molecular and Biotechnology lab, KIRDI, KEMRI, and JKUAT chemistry lab staff for allowing the lab facilities to be used for this research work. The first author also acknowledges Gondar University that gave him supportive material used for this study.

References

- [1] J. M. A. Blair, M. A. Webber, A. J. Baylay, D. O. Ogbolu, and L. J. V. Piddock, "Molecular mechanisms of antibiotic resistance," *Nature Reviews Microbiology*, vol. 13, no. 1, pp. 42–51, 2014.
- [2] K. S. Kaye and J. M. Pogue, "Infections caused by resistant gram-negative bacteria: epidemiology and management," *Pharmacotherapy: The Journal of Human Pharmacology and Drug Therapy*, vol. 35, no. 10, pp. 949–962, 2015.
- [3] C. G. Giske, D. L. Monnet, O. Cars, and Y. Carmeli, "Clinical and economic impact of common multidrug-resistant gram-negative bacilli," *Antimicrobial Agents and Chemotherapy*, vol. 52, no. 3, pp. 813–821, 2008.
- [4] N. Sabtu, D. A. Enoch, and N. M. Brown, "Antibiotic resistance: what, why, where, when and how?" *British Medical Bulletin*, vol. 116, no. 1, pp. 105–113, 2015.
- [5] S. Omulo, S. M. Thumbi, M. K. Njenga, and D. R. Call, "A review of 40 years of enteric antimicrobial resistance research in Eastern Africa: what can be done better?.: What can be done better?" *Antimicrobial Resistance and Infection Control*, vol. 4, no. 1, pp. 1–13, 2015.
- [6] M. E. Ibrahim, N. E. Bilal, and M. E. Hamid, "Increased multi-drug resistant *Escherichia coli* from hospitals in Khartoum state, Sudan," *African Health Sciences*, vol. 12, no. 3, pp. 368–375, 2012.
- [7] D. Lin, K. Chen, E. Wai-Chi Chan, and S. Chen, "Increasing prevalence of ciprofloxacin-resistant food-borne *Salmonella* strains harboring multiple PMQR elements but not target gene mutations," *Scientific Reports*, vol. 5, no. 1, pp. 1–8, 2015.
- [8] F. Jafari, M. Hamidian, M. Rezadehbashi et al., "Prevalence and antimicrobial resistance of diarrheagenic *Escherichia coli* and *Shigella* species associated with acute diarrhea in Tehran, Iran," *Journal of Infectious Disease and Medical Microbiology*, vol. 20, no. 3, pp. e56–e62, 2009.
- [9] S. Prabhu and E. K. Poullose, "Silver nanoparticles: mechanism of antimicrobial action, synthesis, medical applications, and toxicity effects," *International Nano Letters*, vol. 2, no. 32, pp. 1–10, 2012.
- [10] R. S. Prakasham, B. S. Kumar, Y. S. Kumar, and G. G. Shankar, "Characterization of silver nanoparticles synthesized by using marine isolate *Streptomyces albidoflavus*," *Journal of Microbiology and Biotechnology*, vol. 22, no. 5, pp. 614–621, 2012.
- [11] S. Wagi and A. Ahmed, "Bacterial nanobiotic potential," *Green Processing and Synthesis*, vol. 9, no. 1, pp. 203–211, 2020.
- [12] A. Bakhtiari-Sardari, M. Mashreghi, H. Eshghi, F. Behnam-Rasouli, E. Lashani, and B. Shahnavaaz, "Comparative evaluation of silver nanoparticles biosynthesis by two cold-tolerant *Streptomyces* strains and their biological activities," *Biotechnology Letters*, vol. 42, no. 10, pp. 1985–1999, 2020.
- [13] A. A. Hamed, H. Kabary, M. Khedr, and A. N. Emam, "Antibiofilm, antimicrobial and cytotoxic activity of extracellular green-synthesized silver nanoparticles by two marine-derived actinomycete," *RSC Advances*, vol. 10, no. 17, pp. 10361–10367, 2020.
- [14] C. Barros, S. Fulaz, D. Stanicic, and L. Tasic, "Biogenic nanosilver against multidrug-resistant bacteria (MDRB)," *Antibiotics*, vol. 7, no. 3, pp. 69–24, 2018.
- [15] P. Golinska, M. Wypij, A. P. Ingle, I. Gupta, H. Dahm, and M. Rai, "Biogenic synthesis of metal nanoparticles from actinomycetes: biomedical applications and cytotoxicity," *Applied Microbiology and Biotechnology*, vol. 98, no. 19, pp. 8083–8097, 2014.

- [16] P. Manivasagan, J. Venkatesan, K. Sivakumar, and S.-K. Kim, "Actinobacteria mediated synthesis of nanoparticles and their biological properties: a review," *Critical Reviews in Microbiology*, vol. 42, no. 2, pp. 1-13, 2016.
- [17] H. M. Abd-Elnaby, G. M. Abo-Elala, U. M. Abdel-Raouf, and M. M. Hamed, "Antibacterial and anticancer activity of extracellular synthesized silver nanoparticles from marine *Streptomyces rochei* MHM13," *The Egyptian Journal of Aquatic Research*, vol. 42, no. 3, pp. 301-312, 2016.
- [18] R. Chauhan, A. Kumar, and J. Abraham, "A biological approach to synthesis of silver nanoparticles with *Streptomyces* sp JAR1 and its antimicrobial activity," *Scientia Pharmaceutica*, vol. 81, no. 2, pp. 607-621, 2013.
- [19] R. S. Prakasham, B. S. Kumar, Y. S. Kumar, and K. P. Kumar, "Production and characterization of protein encapsulated silver nanoparticles by marine isolate *Streptomyces parvulus* SSNP11," *Indian Journal of Microbiology*, vol. 54, no. 3, pp. 329-336, 2014.
- [20] M. Wypij, J. Czarnecka, M. Świecimska, H. Dahm, M. Rai, and P. Golinska, "Synthesis, characterization and evaluation of antimicrobial and cytotoxic activities of biogenic silver nanoparticles synthesized from *Streptomyces xinghaiensis* OF1 strain," *World Journal of Microbiology and Biotechnology*, vol. 34, no. 2, pp. 1-13, 2018.
- [21] A. Muleta and F. Assefa, "Isolation and screening of antibiotic producing actinomycetes from the rhizosphere and agricultural soils," *African Journal of Biotechnology*, vol. 17, pp. 700-714, 2018.
- [22] A. Bizuye, C. Bii, C. Bii, G. Erastus, and N. Maina, "Antibacterial metabolite prospecting from Actinomycetes isolated from waste damped soils from Thika, central part of Kenya," *Asian Pacific Journal of Tropical Disease*, vol. 7, no. 12, pp. 757-764, 2017.
- [23] A. Bizuye, F. Moges, and B. Andualem, "Isolation and screening of antibiotic producing actinomycetes from soils in Gondar town, North West Ethiopia," *Asian Pacific Journal of Tropical Disease*, vol. 3, no. 5, pp. 375-381, 2013.
- [24] M. Kibret, J. F. Guerrero-Garzón, E. Urban et al., "Streptomyces spp from Ethiopia producing antimicrobial compounds: characterization via bioassays, genome analyses, and mass spectrometry," *Frontiers in Microbiology*, vol. 9, pp. 1-13, 2018.
- [25] M. C. Rotich, E. Magiri, C. Bii, and N. Maina, "Bio-Prospecting for broad spectrum antibiotic producing actinomycetes isolated from virgin soils in kericho county, Kenya," *Advances in Microbiology*, vol. 07, no. 1, pp. 56-70, 2017.
- [26] M. Składanowski, M. Wypij, D. Laskowski, P. Golińska, H. Dahm, and M. Rai, "Silver and gold nanoparticles synthesized from *Streptomyces* sp. isolated from acid forest soil with special reference to its antibacterial activity against pathogens," *Journal of Cluster Science*, vol. 28, no. 1, pp. 59-79, 2017.
- [27] P. S. Kumar, C. Balachandran, V. Duraipandian, D. Ramasamy, S. Ignacimuthu, and N. A. Al-dhabi, "Extracellular biosynthesis of silver nanoparticle using *Streptomyces* sp. 09 PBT 005 and its antibacterial and cytotoxic properties," *Applied Nanoscience*, vol. 5, pp. 169-180, 2015.
- [28] R. A. Ataee, A. Mehrabi-Tavana, S. M. J. Hosseini, K. Moridi, and M. G. Zadegan, "A method for antibiotic susceptibility testing: applicable and accurate," *Jundishapur Journal of Microbiology*, vol. 5, no. 1, pp. 341-345, 2012.
- [29] Q. Li, X. Chen, Y. Jiang, and C. Jiang, "Morphological identification of actinobacteria," in *Actinobacteria-Basics and Biotechnological Applications*, D. Dhanasekaran and Y. Jiang, Eds., pp. 60-86, IntechOpen, London, UK, 2016.
- [30] S. Bowman, P. Roffey, D. McNevin, and M. E. Gahan, "Evaluation of commercial DNA extraction methods for biosecurity applications," *Australian Journal of Forensic Sciences*, vol. 48, no. 4, pp. 407-420, 2016.
- [31] P. Monciardini, M. Sosio, L. Cavaletti, C. Chiocchini, and S. Donadio, "New PCR primers for the selective amplification of 16S rDNA from different groups of actinomycetes1," *FEMS Microbiology Ecology*, vol. 42, no. 3, pp. 419-429, 2002.
- [32] X. Chen, Y. Jiang, Q. Li, L. Han, and C. Jiang, "Molecular phylogenetic identification of actinobacteria xiu," *Actinobacteria-Basics and Biotechnological Applications*, vol. 56, pp. 141-174, 2017.
- [33] D. A. Benson, I. Karsch-Mizrachi, K. Clark, D. J. Lipman, J. Ostell, and E. W. Sayers, "GenBank," *Nucleic Acids Research*, vol. 40, no. D1, pp. D48-D53, 2012.
- [34] S.-H. Yoon, S.-M. Ha, S. Kwon et al., "Introducing EzBioCloud: a taxonomically united database of 16S rRNA gene sequences and whole-genome assemblies," *International Journal of Systematic and Evolutionary Microbiology*, vol. 67, no. 5, pp. 1613-1617, 2017.
- [35] L. Karthik, G. Kumar, A. V. Kirthi, A. A. Rahuman, and K. V. Bhaskara Rao, "Streptomyces sp. LK3 mediated synthesis of silver nanoparticles and its biomedical application," *Bioprocess and Biosystems Engineering*, vol. 37, no. 2, pp. 261-267, 2014.
- [36] Y. K. Mohanta and S. K. Behera, "Biosynthesis, characterization and antimicrobial activity of silver nanoparticles by *Streptomyces* sp. SS2," *Bioprocess and Biosystems Engineering*, vol. 37, no. 11, pp. 2263-2269, 2014.
- [37] N. E.-A. El-Naggar, N. A. M. Abdelwahed, and O. M. M. Darwesh, "Fabrication of biogenic antimicrobial silver nanoparticles by *Streptomyces aegyptia* NEAE 102 as eco-friendly nanofactory," *Journal of Microbiology and Biotechnology*, vol. 24, no. 4, pp. 453-464, 2014.
- [38] S. A. Ibrahim, S. K. Abd-El-Aal, A. AG, and M. A. El-Sayd, "Molecular identification and characterization of some gluconacetobacter strains isolated from some Egyptian fruits," *Research Journal of Pharmaceutical, Biological and Chemical Sciences*, vol. 5, no. 4, pp. 1617-1627, 2014.
- [39] M. Kontro, U. Lignell, M.-R. Hirvonen, and A. Nevalainen, "pH effects on 10 *Streptomyces* spp growth and sporulation depend on nutrients," *Letters in Applied Microbiology*, vol. 41, no. 1, pp. 32-38, 2005.
- [40] J. Yang, Z. Yang, Y. Yin, M. Rao, Y. Liang, and M. Ge, "Three novel polyene macrolides isolated from cultures of *Streptomyces lavenduligriseus*," *The Journal of Antibiotics*, vol. 69, no. 1, pp. 62-65, 2015.
- [41] A. Sarmiento-Vizcaíno, A. F. Braña, V. González et al., "Atmospheric dispersal of bioactive *Streptomyces* albido-flavus strains among terrestrial and marine environments," *Microbial Ecology*, vol. 71, no. 2, pp. 375-386, 2015.
- [42] J. Y. Lee, J. Y. Lee, H. W. Jung, and B. K. Hwang, "*Streptomyces koyangensis* sp. nov., a novel actinomycete that produces 4-phenyl-3-butenic acid," *International Journal of Systematic and Evolutionary Microbiology*, vol. 55, no. 1, pp. 257-262, 2005.
- [43] M. Kulkarni, S. Gorthi, G. Banerjee, and P. Chattopadhyay, "Production, characterization and optimization of actinomycin D from *Streptomyces hydrogenans* IB310, a (n antagonistic bacterium against phytopathogens," *Biocatalysis and Agricultural Biotechnology*, vol. 10, pp. 69-74, 2017.

- [44] S. M. Pimentel-Elardo, S. Kozytska, T. S. Bugni, C. M. Ireland, H. Moll, and U. Hentschel, "Anti-parasitic compounds from *Streptomyces* sp. strains isolated from Mediterranean sponges," *Marine Drugs*, vol. 8, no. 2, pp. 373–380, 2010.
- [45] P. Caffrey, S. Lynch, E. Flood, S. Finnan, and M. Oliynyk, "Amphotericin biosynthesis in *Streptomyces nodosus*: deductions from analysis of polyketide synthase and late genes," *Chemistry & Biology*, vol. 8, no. 7, pp. 713–723, 2001.
- [46] P. Sweeney, C. D. Murphy, and P. Caffrey, "Exploiting the genome sequence of *Streptomyces nodosus* for enhanced antibiotic production," *Applied Microbiology and Biotechnology*, vol. 100, no. 3, pp. 1285–1295, 2016.
- [47] T. M. Nguyen and J. Kim, "Description of *Streptomyces fabae* sp. nov., a producer of antibiotics against microbial pathogens, isolated from soybean (*Glycine max*) rhizosphere soil," *International Journal of Systematic and Evolutionary Microbiology*, vol. 65, no. Pt_11, pp. 4151–4156, 2015.
- [48] H. Matsuo, Y. Kondo, T. Kawasaki, and N. Imamura, "Cineromycin B isolated from *Streptomyces cineromogenes* inhibits adipocyte differentiation of 3T3-L1 cells via Krüppel-like factors 2 and 3," *Life Sciences*, vol. 135, pp. 35–42, 2015.